Materials Science Forum Vols 527-529 (2006) pp 689-694 *Online: 2006-10-15*

doi:10.4028/www.scientific.net/MSF.527-529.689

Phonons in SiC from INS, IXS, and Ab-Initio Calculations

D. Strauch[1,a], B. Dorner[2,b], A. Ivanov[2,c], M. Krisch[3,d], J. Serrano[3,e], A. Bosak[3,f], W. J. Choyke[4,g], B. Stojetz[1,h] and M. Malorny[1,i]

[1]Institut für Theoretische Physik, Universität Regensburg, D-93040 Regensburg, Germany

[2]Institut Laue-Langevin, BP 156, F-38042 Grenoble Cedex 9, France

[3]European Synchrotron Radiation Facility, BP 220, F-38043 Grenoble Cedex 9, France

[4]Department of Physics, University of Pittsburgh, Pittsburgh PA 15260, USA

[a]dieter.strauch@physik.uni-regensburg.de, [b]dorner@ill.fr, [c]aivanov@ill.fr, [d]krisch@esrf.fr, [e]jserrano@esrf.fr, [f]bossak@esrf.fr, [g]choyke+@pitt.edu, [h]bernhard.stojetz@physik.uni-regensburg.de, [i]michael.malorny@physik.uni-regensburg.de

Keywords: phonon dispersion, inelastic neutron scattering, inelastic X-ray scattering, scattering intensity, ab initio calculation, 3C-SiC, 4H-SiC

Abstract. Preliminary results for the phonon dispersion curves of hexagonal 4H-SiC from experimental inelastic neutron (INS) and X-ray scattering (IXS) are reported and contrasted with those of cubic 3C-SiC and silicon. The experimental frequencies and scattering intensities are in excellent agreement with those from first-principles calculations using density-functional methods. The relative merits of the two experimental techniques and aspects of the density functional perturbation theory and the so-called frozen phonon method for the determination of the basic phonon properties are briefly outlined.

Introduction

SiC is a wide band gap semiconductor of particular interest for opto-electronic devices and high-power, high-temperature applications. It exists in many different crystallographic forms, amongst which some hexagonal (for example 6H) and rhombohedral modifications are the most abundant ones, while the cubic 3C and hexagonal 4H modifications are of main interest at present.

The present paper deals with phonons as the only grounds on which the thermal properties of non-defective SiC rest. From the standpoint of phonon physics the cubic 3C modification with just one formula unit (two atoms) is the most simple one with six phonon dispersion branches ($6 = 2 \times 3$, two atoms, each with three degrees of freedom). In contrast, 4H-SiC with four formula units (eight atoms) poses serious problems since the present-day resolution in INS and IXS often is not sufficient to resolve the 24 closely lying dispersion branches which are within the same energy range as the six branches of 3C-SiC. This problem can be circumvented by Raman scattering, which provides a much better energy resolution, but yields only phonon frequencies of Raman-active, optical modes at the Brillouin-zone (BZ) center.

In recent years, model calculations of phonon dispersion curves have been replaced by first-principles techniques, if applied to systems with a small number of atoms (up to 20 or so) per elementary cell. For most systems these calculations yield very reliable results, when compared to available experimental data. In addition, a-priori calculations give useful assistance in the planning of experiments and in the effective use of the valuable beam time of neutron or synchrotron facilities.

The phonon dispersion curves of 3C-SiC from first-principles calculations [1] had preceded their experimental verification [2]; the acoustic-mode frequencies extend up to about 75 meV, and the optic-mode frequencies ly in the region between about 90 and 125 meV. A limited set of experimental data of 4H-SiC together with ab-initio dispersion curves has been published [3] and extended recently [4].

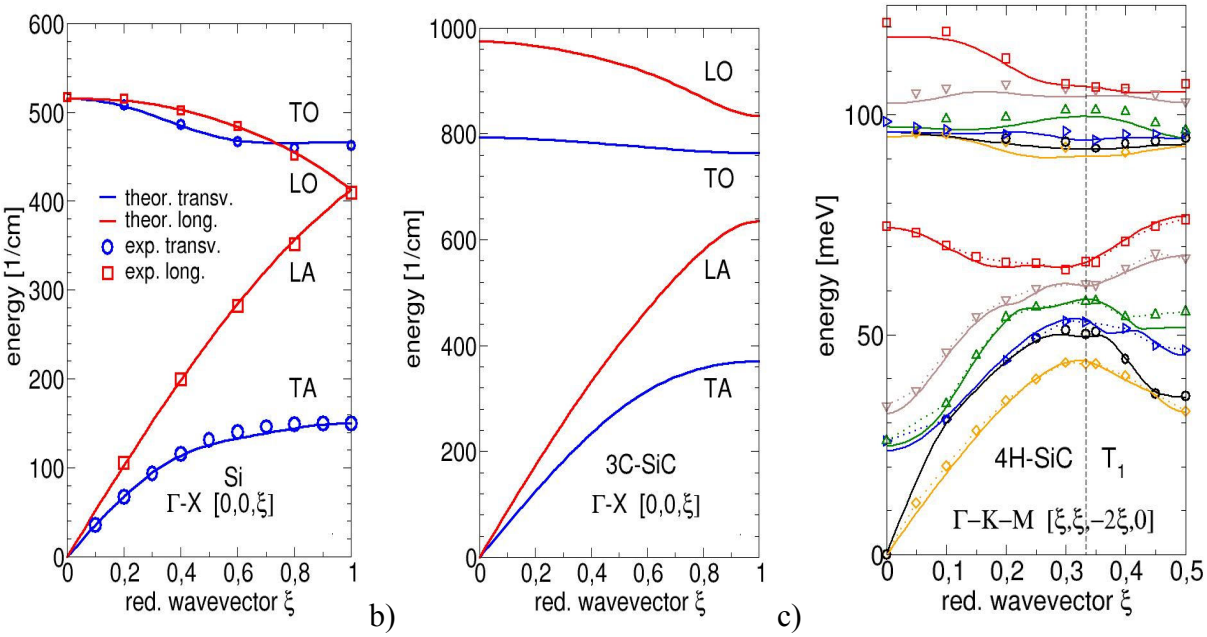

Fig. 1: Phonon dispersion curves in Si (a), 3C-SiC (b), and 4H-SiC (c). For clarity, only the T_1-mode dispersion curves are shown for 4H-SiC. The data points of 4H-SiC below 80 meV and above 90 meV are from INS and IXS experiments, respectively. The lines are from ab-initio calculations.

Fig. 1 shows a selection of dispersion curves of Si, 3C-SiC, and 4H-SiC. There are systematic differences between the phonons of an elemental semiconductor like Si and of 3C-SiC, both of the same tetrahedral coordination: Due to the partially ionic character of SiC, there is an LO-TO splitting of the optical modes at the center of the BZ, which is absent in Si, and due to the two different masses in SiC the (partial) degeneracy at the BZ boundary is lifted (see left and middle panels of Fig. 1.) -- Due to the four times larger lattice constant in 4H-SiC in the stacking direction the extent of the BZ in that direction is four times smaller and the number of phonon modes is four times larger, (see middle and right panels of Fig. 1). In this contribution we will deal with the methods of how the theoretical and experimental phonon dispersion curves for SiC have been obtained.

Experimental

Inelastic Scattering. The general method is that of inelastic scattering of probe particles, which were neutrons or synchrotron X-ray photons in our experiments. The incoming probe has energy E_i and wave vector $\boldsymbol{k}_i$ (momentum $h\boldsymbol{k}_i/2\pi$); the outgoing probe is analyzed in terms of energy E_f and wave vector $\boldsymbol{k}_f$; the differences

$$E = E_i - E_f \quad \text{and} \quad \boldsymbol{Q} = \boldsymbol{k}_i - \boldsymbol{k}_f$$

are taken up by a phonon (higher-order processes are less probable) with wave vector $\boldsymbol{q} = \boldsymbol{Q} - \boldsymbol{g}$ and by the crystal as a whole described by a reciprocal lattice vector $\boldsymbol{g}$ as sketched in Fig. 2. By scanning the energy at a given wave vector (momentum) the maximum scattered intensity occurs at the energy of the phonon (at that wave vector $\boldsymbol{q}$) as sketched in Fig. 3.

Raman and Brillouin Scattering. In relation to INS and IXS, in standard Raman or Brillouin scattering the momenta k_i and k_f of the visible light are so small that $Q \sim 0$ and thus $q \sim 0$, and only modes (optical modes in Raman, acoustic modes in Brillouin scattering) with wave vector very close to the center of the BZ can be investigated, but with higher precision than for INS or IXS.

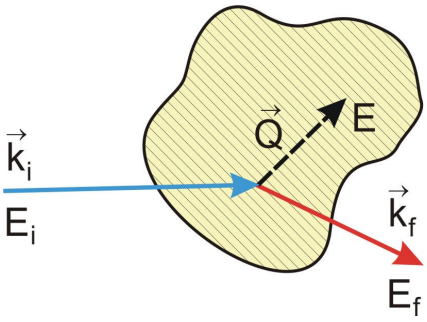

Fig. 2: Schematic representation of the inelastic scattering process.

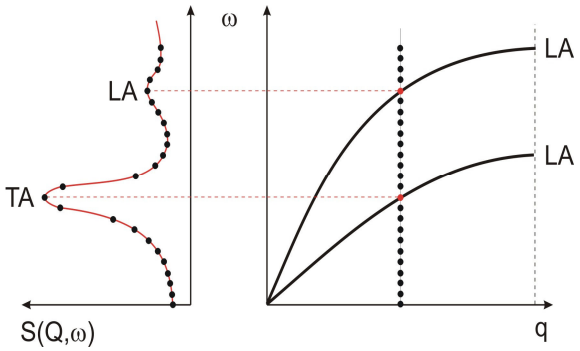

Fig. 3: Schematic constant-Q scan: For various frequencies at a given $\boldsymbol{q}$ (indicated by the dots in the right part) counts $S(\boldsymbol{q},\omega)$ are taken (as indicated in the left part).

INS and IXS. In contrast to the former, the typical wave vectors in INS and IXS are in the Å^{-1} regime, and the transferred momentum is taken up by the phonon (or any other elementary excitation) *and* the crystal lattice as a whole (called Umklapp process in other contexts). This makes wave vectors from anywhere of the BZ accessible. As in Raman or Brillouin scattering small sample volumes, ranging from 10^{-4} to 1 mm^3, are sufficient for IXS. In contrast, INS requires a sample size of cm^3 or above for sufficiently high inelastic scattering rates. Depending on the nuclear isotopes INS sometimes suffers from large absorption or incoherent cross-sections, the latter being absent in IXS, where photons are scattered from the electrons rather than from the nuclei. A disadvantage of IXS may be the small coupling constant (the atomic form factor) of the lighter elements. For further details see Ref. [5].

INS. The neutron data have been recorded on the instrument IN1 of the Institut Laue-Langevin (ILL). Due to the unavailability of the hot source at the time of the first experiment only the phonon branches up to 75 meV could be investigated. The Cu(220) reflecting planes were used as monochromator and analyzer. The 30' Soller slit collimators have been installed after monochromator, sample, and analyzer. Constant-$\boldsymbol{Q}$ scans have been taken with fixed final momentum between $k_f = 5.0$ Å^{-1} and $k_f = 5.75$ Å^{-1}; these high values were chosen for kinematical reasons and to avoid spurious effects, which were to be expected at lower values of k_f. The crystal with a size of 24×24×18 mm^3 was cooled to around 11 K to reduce multi-phonon background scattering. The phonon modes with wave vectors along the Γ-M and Γ-K-M (from the BZ center to boundaries), and K-H, M-L, and A-H-L directions (along BZ boundaries) have been investigated.

When the hot neutron source became available again, some additional days have been devoted to the high-frequency modes of T_2 symmetry along the Γ-K-M direction. The monochromator was Cu(331), and the analyzer was Cu(220). The collimator, set open-60'-60'-60', was used initially for the high-intensity runs and reduced later to open-20'-20'-20' in order to considerably improve the resolution (down to about 4 meV) at the expense of strongly reduced count rates. The final momentum in this experiment was $k_f = 6.279$ Å^{-1}.

IXS. The X-ray data have been recorded on the instrument ID28 of the European Synchrotron Radiation Facility (ESRF), using the silicon (9 9 9) set-up, which gives an energy of 17.794 keV and a wave vector of ~9 Å^{-1} with an overall experimental energy resolution of 3 meV and a momentum resolution of 0.013 Å^{-1} (FWHM). The crystal had a size of 5×3×0.2 mm^3 with the surface normal along [1,1,-2,0]. The high-frequency modes with wave vectors along Γ-K-M (from the BZ center to the boundary, T_2-symmetry modes only), M-L, and A-H-L (along BZ boundaries) have been investigated at ambient temperature. The trivial modes with wave vectors along the Γ-A direction have not been investigated in either method. Results will be presented below.

The Scattering Intensity. The scattering intensity (or cross-section) for Stokes scattering is related to the scattering function

$$S(\boldsymbol{Q},\omega) = \sum_{\boldsymbol{Q},g,q,j} |\sum_{\kappa} a_{\kappa}(\boldsymbol{Q},\boldsymbol{q},j)|^2 \, \delta(\boldsymbol{q}+\boldsymbol{g}-\boldsymbol{Q}) \, \delta(\omega(\boldsymbol{q},j)-\omega) \, [1+n(\omega)]/\omega$$

$$a_\kappa(\boldsymbol{Q},\boldsymbol{q},j) = f_\kappa(\boldsymbol{Q})\ \boldsymbol{Q}\cdot\boldsymbol{u}_\kappa(\boldsymbol{q},j)\ \exp(-i\boldsymbol{Q}\cdot\boldsymbol{R}_\kappa)\ \exp(-W_\kappa)\ .$$

Here, $a_\kappa(\boldsymbol{Q},\boldsymbol{q},j)$ is the scattering amplitude, κ labels the atoms in the elementary cell; $f_\kappa(\boldsymbol{Q})$ is the electronic form factor in the case of IXS and equal to the $\boldsymbol{Q}$-independent scattering length b_κ in the case of INS; $\boldsymbol{R}_\kappa$ is the atom position within the elementary cell; W_κ is the Debye-Waller (temperature) factor, which we have neglected in our calculations; the two delta functions account for energy and momentum conservation, respectively; $n(\omega)$ is the Bose factor. A-priori calculation of the scattering intensity assists in planning the experiment which requires the determination of the phonon eigen frequencies $\omega(\boldsymbol{q},j)$ and eigenvectors $\boldsymbol{u}_\kappa(\boldsymbol{q},j)$ as will be described in the following.

Theoretical

With eight atoms per elementary cell ab-initio investigations of 4H-SiC are feasible. The general procedure contains two steps. The phonon properties depend on the inter-atomic bonding, which is mediated by the electrons. Thus, the first step is the determination of the electronic properties. With these results as an input the phonon properties can be investigated in a second step.

Electronic Ground-State Calculations. There are two basically different approaches, the Hartree-Fock (HF) method and the density functional theory (DFT). While in the HF method correlation is neglected (except for extensions with the so-called configuration interaction), it is, in principle, included in DFT. However, the correlation-and-exchange operator in DFT is not known, but there are approximations tested for their applicability. While the HF equations are coupled one-electron equations, the Kohn-Sham equations of DFT for one-electron wave functions are decoupled from each other.

Ab-initio Pseudopotentials. The chemical bond between atoms is mostly caused by their respective valence electrons in the overlap region; the core electrons contribute little (there are means of taking them into account). In order to reduce numerical work ab-initio pseudopotentials are employed: Typically, a pseudopotential of an *isolated* atom is constructed such that the pseudo energies agree with the true valence energies and that the valence wave functions in the outer region (essentially beyond their main maximum) agree with the true functions; in the core region a smoothly varying function is chosen. With this pseudopotential introduced into the crystalline structure, the expansion of the total, relatively smooth wave functions in terms of plane waves is feasible.

Computer Codes (DFT and HF). There is a number of codes available, mostly for periodic systems. Our own experience is with VASP [6], Abinit [7], PWscf [8] (DFT codes based on plane-wave expansions and pseudopotentials), and an earlier version of Wien2k [9] (a full-potential DFT code based on LAPW functions and local orbitals). All these codes employ either the (spin) local density (L(S)DA) or generalized gradient approximation (GGA) for the exchange-and-correlation functional. There are further codes like CASTEP [10] (a DFT code based on plane waves and pseudopotentials) or SIESTA [11] (a DFT code based on atomic orbitals).

Frozen-Phonon Method. Before the advent of the density functional perturbation theory (DFPT, or response theory) one calculated the total energy as a function of atomic displacements and took differences to calculate forces and hence the phonon frequencies as sketched in Fig. 4,

$$F = -\Delta E / \Delta u \quad \text{and} \quad m\omega^2 = D = -\Delta F / \Delta u = \Delta E^2 / \Delta u^2.$$

Since the atomic displacements change the crystal symmetry, super-cell calculations are necessary, and, therefore, only a few phonons with highly symmetrical wave vectors can be treated. Also, the eigenvectors often are not known a priori. Finally, the LO-TO splitting is usually not obtained. The advantage, however, is the fact that the forces are not restricted to the harmonic part as in DFPT.

Density Functional Perturbation Theory (DFPT). The essential quantity in DFT is the one-electron density, and in DFPT the first-order change of the one-electron wave function (and quantities derived thereof) per unit displacement *at the equilibrium position* is calculated,

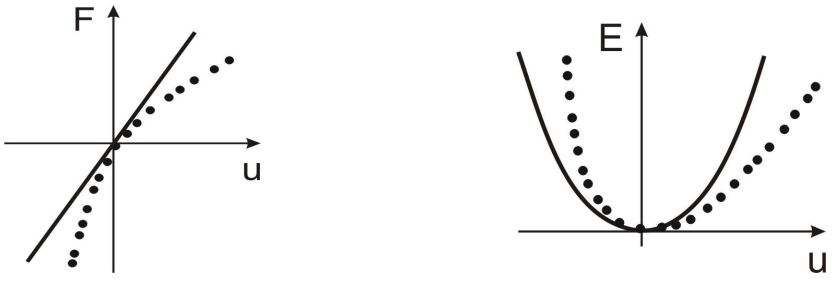

Fig. 4: The force F and the (total) energy E as a function of the displacement u (dots) and the fit to Hooke's law (curves) (schematical).

$$F = -\,dE/du\,\big|_{u=0} \quad \text{and} \quad m\omega^2 = D = dE^2/du^2\,\big|_{u=0}\,.$$

For a review, see Ref. [12]. Thus, the crystal structure is maintained in the computation which allows the use of symmetry operations of the undeformed crystal. Actually, the complete so-called dynamical matrix $\boldsymbol{D}(\boldsymbol{q})$ (of dimension 24×24 in the case of 4H-SiC) for a given phonon wave vector $\boldsymbol{q}$ is obtained, and from the diagonalization of $\boldsymbol{D}(\boldsymbol{q})$ one obtains the complete set of frequencies $\omega(\boldsymbol{q}j)$ and eigenvectors $\boldsymbol{u}_\kappa(\boldsymbol{q}j)$. In contrast to the frozen-phonon method essentially *any* wave vector $\boldsymbol{q}$ is accessible.

Computer Codes (DFPT). In addition to the ground-state properties, the Abinit [7] and PWscf [8] computer codes allow the calculation not only of dynamical matrices but also of the effective charges, high-frequency dielectric constants, and other quantities and are permanently updated and their applications extended. In particular the Abinit code is extensively documented, and people with relatively little computer experience can handle these programs. From the PHONON code [13] phonon dispersion curves and densities of states for crystals from empirical force constants or DFT forces can be calculated.

Results

Even without numerical calculations symmetry arguments are of help, if the phonon wave vector is along a direction of high symmetry, since in this case the excitation of phonons of particular symmetries may be forbidden in one or another BZ. This is why dispersion curves are often, and in our case as well, taken along high-symmetry wave-vector directions.

The upper panels of Fig. 5 show typical INS and IXS scans, respectively, from the high-frequency region. In both cases the phonon wave vector is $\boldsymbol{q}$ = (0.3, 0.3, 0) $2\pi/a$ in the Γ-K-M direction. With the symmetry of the total momentum transfer $\boldsymbol{Q}$ = (h, h, l) only the modes of T_1 (T_2) symmetry are visible for l even (l odd); these are 12 modes for each symmetry with 6 each in the low- and high-frequency region. Also shown are more or less unbiased fits with the instrumental Gaussian (INS) or Lorentzian (IXS) resolution functions. Due to the close spacing the six modes in each spectrum cannot be resolved, except possibly for the gap between the low- and high-frequency modes. Taking spectra for a given $\boldsymbol{q} = \boldsymbol{Q} - \boldsymbol{g}$, but with different $\boldsymbol{g}$, different (relative) scattering intensities are recorded because of the phase factor $\exp(-i\boldsymbol{Q}\cdot\boldsymbol{R}_\kappa)$ and the scalar product $\boldsymbol{Q}\cdot\boldsymbol{u}_\kappa(\boldsymbol{q}j)$ in the scattering amplitude $a_\kappa(\boldsymbol{Q},\boldsymbol{q}j)$ above, and if a sufficiently large number of them are collected, one may be able to determine the different frequencies; this is the standard way, and to this end an extensive search program is set up in many cases.

In order to avoid any unsuccessful search of this kind a-priori calculations are of help. In the present case of 4H-SiC (and even more so for 3C-SiC) we have made very reliable DFPT calculations for the phonon eigen frequencies and eigenvectors, and from those we have calculated the (relative) scattering intensities for different, experimentally accessible momentum transfers $\boldsymbol{Q}$. Out of the resulting list of scattering intensities we have selected those $\boldsymbol{g}$, which give large intensities for some modes and small ones for the neighboring ones, even though this may not

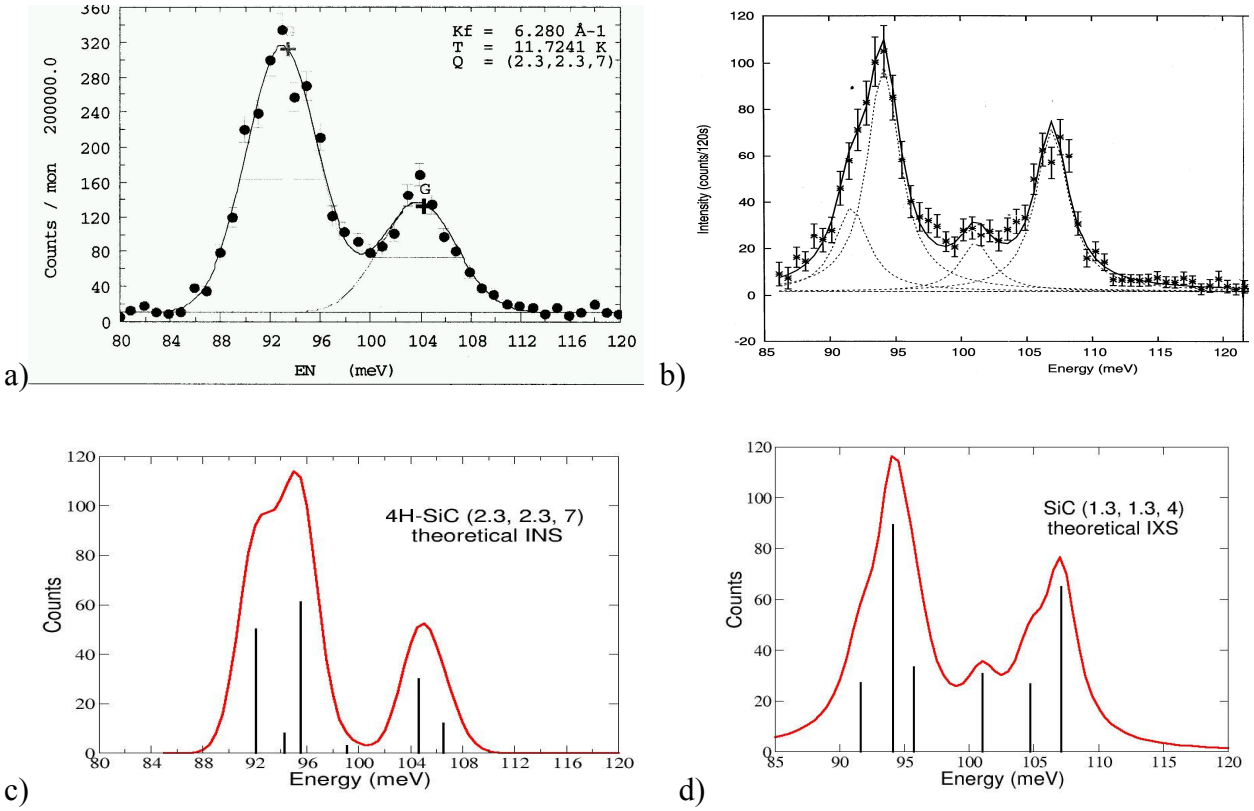

Fig. 5: INS scattering spectrum of T_1-symmetry modes (a) and IXS spectrum of T_2-symmetry modes (b) for phonon wave vector $\boldsymbol{q}$ = (0.3, 0.3, 0) $2\pi/a$ in the high-frequency region. Panels (c) and (d) show the simulation of these data with phonon input from ab-initio calculations with a Gaussian width of 4 meV for the INS case and a Lorentzian width of 3 meV for the IXS case. The figures are scaled such that the energies and (arbitrary) intensities approximately match for each of the two sets.

always be possible. Putting the results for the T_1-symmetry modes together one arrives at the results shown in the right panel of Fig. 1.

Summary

Experimental and theoretical results for phonon frequencies as well as for scattering intensities are in excellent agreement. This shows that present-day DFT-based computations are very reliable and that the LDA used is a valid approximation for the present system. In addition, the experimental intensities can be assigned very safely, even if unresolved. A more complete account with further results will be published separately [4].

References

[1] K. Karch et al.: Phys. Rev. B Vol. 50 (1994), p. 17054, Int. J. Quantum Chem. Vol. 56 (1995), p. 801.
[2] J. Serrano et al.: Appl. Phys. Letters Vol. 80 (2002), p. 4360.
[3] J. Serrano et al.: Mater. Sci. Forum Vol. 257 (2003), p. 433.
[4] D. Strauch et al.: to be published.
[5] E. Burkel, *Inelastic Scattering of X-Rays with Very High Energy Resolution,* Springer Tracts in Modern Physics, Vol. 125 (1991).
[6] http://cms.mpi.univie.ac.at/vasp/vasp/vasp.html
[7] http://www.abinit.org
[8] http://www.pwscf.org
[9] http://www.WIEN2k.at
[10] http://www.tcm.phy.cam.ac.uk
[11] http://www.uam.es/departamentos/ciencias/fismateriac/siesta
[12] S. Baroni, S. de Gironcoli, A. Dal Corso and P. Giannozzi: Rev. Mod. Phys. Vol. 73 (2001), p. 515.
[13] http://wolf.ifj.edu.pl/phonon/

Silicon Carbide and Related Materials 2005
10.4028/www.scientific.net/MSF.527-529

Phonons in SiC from INS, IXS, and Ab-Initio Calculations
10.4028/www.scientific.net/MSF.527-529.689

DOI References
[5] E. Burkel, Inelastic Scattering of X-Rays with Very High Energy Resolution, Springer Tracts in Modern Physics, ol. 125 (1991).
doi:10.1007/BFb0045866
[12] S. Baroni, S. de Gironcoli, A. Dal Corso and P. Giannozzi: Rev. Mod. Phys. Vol. 73 (2001), p. 515.
doi:10.1103/RevModPhys.73.515